Roof- and Pyramid Wavefront Sensing with Blurred Sources

Brent Ellerbroek[1], Jean-Pierre Veran[2], Lianqi Wang[3]

[1]Retired
[2]NRC Herzberg Institute of Astrophysics
[3]Thirty Meter Telescope International Observatory

Abstract

We generalize the standard Fourier optics measurement equations for the roof- and pyramid wavefront sensor (RWFS and PWFS) concepts to the case of blurred (non-point) sources. Samples of blurred sources include (i) extended astronomical objects such as moons, (ii) point sources with modulation (i.e., tip/tilt nutation), and (iii) elongated laser guide stars. For simple source profiles, for example top-hat or Gaussian functions, the effect of the blurring on the measurement can be represented analytically as a filter function for each of these sample cases. For the RWFS, we use this representation to evaluate the impact of source blurring on the measurement error due to noise, as a function of the number of Zernike modes estimated. A limited set of sample results are also presented for more computationally intensive case of the PWFS.

1. Introduction

Intuitively, the sensitivity of the pyramid wavefront sensor (PWFS) is reduced if measurements are made using a blurred or extended object as the guide star, instead of a point source. The purpose of this study is to model this effect analytically, and assess the resulting increase in wavefront reconstruction error due to measurement noise.

We also consider the case of the roof WFS (RWFS). The two-channel RWFS provides a pair of bi-cell wavefront gradient measurements at each point in the pupil, instead of the quad cell gradient measurement obtained with the PWFS.
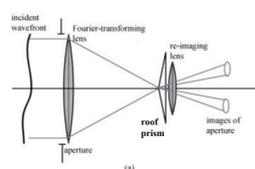
Roof WFS (one of two channel)   Pyramid WFS
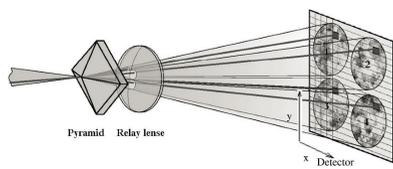
2. RWFS and PWFS Measurement Models with Blurred Sources

The Fourier optics model for the point source gradient measurement g is given by

$$g_{\{x,y\}}(r,\phi) = \sum_i w_{\{x,y\},i} I(r,\phi,m_i)$$

$$I(r,\phi,m) = \left| \int d\kappa \, m(\kappa) \exp\left(\frac{2\pi i}{\lambda} r \cdot \kappa\right) \int ds \, A(s) \exp(i\phi(s)) \exp\left(-\frac{2\pi i}{\lambda} s \cdot \kappa\right) \right|^2 .$$

Here r is a point in the pupil, ϕ is the wavefront, the sum is taken over the 2 or 4 detectors used in the measurement, $w_{\{x,y\},i}$ is the quad-cell (or bi-cell) weight for detector i, m_i is the spatial filtering provided by the pyramid (or roof) for this detector, and $A(s)$ is the pupil function.

For an extended and/or blurred guide star, we model guide star as a superposition of discrete, incoherent point sources, with the wavefront ϕ adjusted by the appropriate tilt and/or focus terms at each point:

$$g_{\{x,y\}}(r,\phi) = \sum_i w_{\{x,y\},i} \int d\theta \, W(\theta) \int df \, p(f) I(r,\phi + \theta_x Z_2 + \theta_y Z_3 + f Z_4, m_i)$$

Here W is the intensity profile of an extended object (or a modulated point source), and p is the vertical profile of an elongated guide star.

If the elongation profile p is simply a top-hat, the RWFS x-gradient measurement can be evaluated as:

$$g_x(r,\phi) = \lambda^4 \int dt_x A(r) A(r+(t_x,0)) \hat{W}(t_x/\lambda) \left[\frac{\sin(\alpha(2r_x t_x + t_x^2))}{\alpha(2r_x t_x + t_x^2)} \right] \left[\frac{\sin(\phi(r) - \phi(r+(t_x,0)))}{\pi t_x} \right]$$

Here α is the peak-to-valley defocus at the edge of the range gate. Sample values of the extended object filter function include:

$$\hat{W}(t/\lambda) = \begin{cases} J_0(\alpha\pi t/2) & \text{Circular modulation of diameter } D_m = \alpha(\lambda/D) \\ \dfrac{4J_1(\alpha\pi t/2)}{\alpha\pi t} & \text{Uniform disk of diameter } D_o = \alpha(\lambda/D) \end{cases}$$

The PWFS x-gradient formula is similar in form, but includes a triple integral:

$$g_x(r,\phi) = \frac{\lambda^4}{2} \int dt_x A(r) A(r+(t_x,0)) \hat{W}(t_x/\lambda) \left[\frac{\sin(\alpha(2r_x t_x + t_x^2))}{\alpha(2r_x t_x + t_x^2)} \right] \left[\frac{\sin(\phi(r) - \phi(r+(t_x,0)))}{\pi t_x} \right]$$

$$- \frac{\lambda^4}{2} \iint \frac{dt_y}{\pi t_y} \frac{dt'_y}{\pi t'_y} \int dt_x A(r+(0,t'_y)) A(r+t)$$

$$\times \hat{W}\left(\frac{|t-(0,t'_y)|}{\lambda} \right) \left[\frac{\sin(\alpha(|r+(0,t'_y)|^2 - |r+t|^2))}{\alpha(|r+(0,t'_y)|^2 - |r+t|^2)} \right] \left[\frac{\sin(\phi(r+(0,t'_y)) - \phi(r+t))}{\pi t_x} \right]$$

3. Influence Matrix Calculations

These RWFS and PWFS models have been used to compute Zernike mode influence matrices. Point source results for Z7 on a 65x65 point pupil are illustrated below:

RWFS and PWFS Measurements of Y-Coma

| | Gradient (for comparison) | RWFS, no modulation | RWFS, 2 λ/D modulation | PWFS, no modulation | PWFS, 2 λ/D modulation |
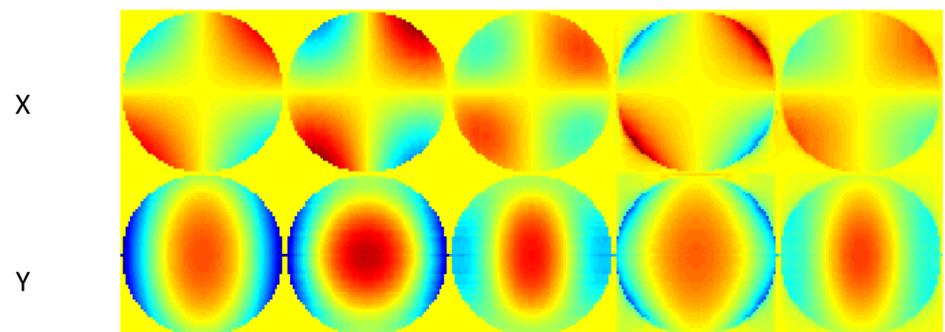
The RWFS and PWFS measurements with no modulation are similar to the analytically computed wavefront gradients (and have also been checked again Fourier optics calculations). The reduction in sensitivity due to source modulation is evident from the figures, and is roughly a factor of two in this case. Similar results have been obtained for extended (disk) source and elongated guide stars.

4. Wavefront Reconstruction Error Due to Noise for the Roof WFS

The Zernike mode influence matrices computed as above can be used to assess the wavefront estimation error due to measurement noise for a nominal unweighted, least squares wavefront reconstruction algorithm. The following plots illustrate the mean-square estimation error due noise as a function of the amount of blurring of the source and the number of Zernike modes estimated, normalized with respect to the error in estimating a single tilt mode with a point source:
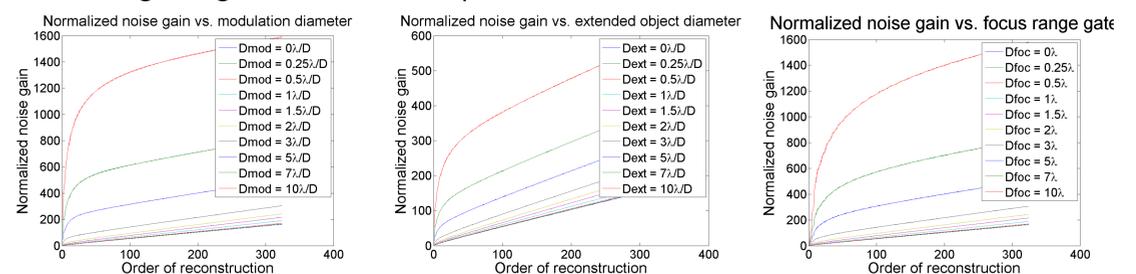
In general, the results illustrate that the effect of object blurring on the reconstruction error due to noise is relatively modest for objects no larger than λ/D, or focus range gates smaller than one wave PV. For larger amount of blurring, the reconstruction error in the low-order modes appears to increase roughly with the square of the blurring.

5. Wavefront Reconstruction Error Due to Noise for the Pyramid WFS

Computing influence matrices for the PWFS is computationally intensive because of the triple integrals to be evaluated. Sample preliminary results computed with 65x65 point pupils indicate that the trends in the reconstruction error due to noise are only qualitatively similar to the RWFS. To be continued…